ANALYSIS OF LOW- AND HIGH-RESOLUTION OBSERVATIONS OF HIGH-VELOCITY CLOUDS

Bart P. Wakker
Kapteyn Laboratorium, Rijks Universiteit Groningen
Postbus 800, 9700AV Groningen, The Netherlands

1. Introduction

For almost three decades neutral hydrogen moving at velocities unexplicable by galactic rotation has been observed. These so-called high-velocity clouds (HVCs) have been invoked as evidence for infall of neutral gas to the galaxy, as manifestations of a galactic fountain, as energy source for the formation of supershells, etc. No general consensus about their origin has presently been reached. However, it is becoming clear that no single model will suffice to explain all HVCs. A number of clouds may consist of material streaming toward the galactic center, as Mirabel (this conference) has advocated for several years, though their origin still remains unclear. A better understanding is mainly hampered by the fact that the distance remains unknown. An overview of the current status of the distance problem is given by van Woerden elsewhere in this volume.

Recently a deep and complete survey of the HV gas has been completed (Hulsbosch & Wakker 1988, Bajaja *et al.* 1985). Older surveys, notably the one by Giovanelli (1980) provided much insight into the phenomenon but suffered from incompleteness. In the new surveys the whole sky north of declination $-18°$ is covered on a $1°\times1°$ grid with a $36'$ beam and a detection limit of 0.05 K (corresponding to about $10^{18}\,\mathrm{cm}^{-2}$) , while south of $-18°$ the grid is $2°\times2°$ with detection limit 0.08 K. In Section 2 one of the new results based on these data is presented, which is related to the absorption-line studies of galactic halo gas. The survey data also allow one to constrain models for the origin of HVCs, as is described in Section 3.

More detailed maps of HVCs have been made since 1973 (Giovanelli, Cram & Verschuur). These data revealed the presence of spatial and velocity fine structure within the clouds. The smallest concentrations were unresolved with the $12'$ to $20'$ beams used. Giovanelli & Haynes (1976) discovered that at this resolution the velocity profile often showed a sharp (FWHM $7\,\mathrm{km\,s}^{-1}$) peak on top of a broad (FWHM $23\,\mathrm{km\,s}^{-1}$) plateau. From 1979 onward data at $1'$ resolution have been taken with the Westerbork synthesis telescope. These are described in Section 4 and show that the intrinsic linewidths are narrower (FWHM $3\,\mathrm{km\,s}^{-1}$) and that the broader profiles are likely to be due to beam smearing.

2. Sky coverage

Figure 1 shows a number of curves $C(T>T_0)$, defined as the percentage of sky area at which HVCs are found with brightness temperature above a certain limit T_0

for a given velocity limit. At the survey limit of 0.05 K 9% of the sky is covered by gas having $|v_{lsr}| > 100\,km\,s^{-1}$, an increase of a factor two when compared to older surveys (with detection limits of the order of 0.2 K).

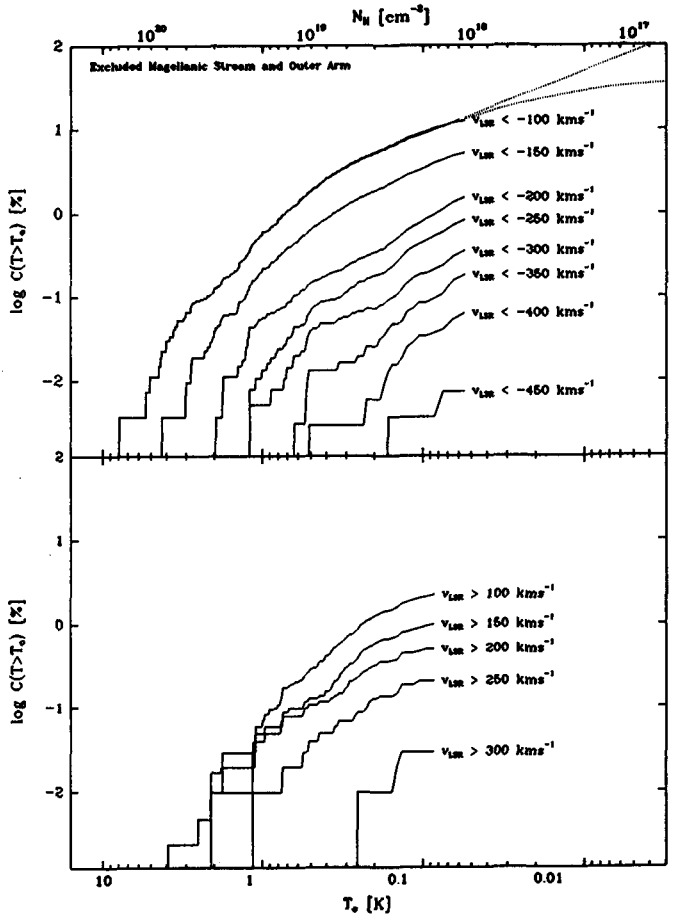

Figure 1. Each curve shows the percentage of sky area covered by high-velocity gas with velocity above the indicated limit as function of detection limit. The lower x-scale is in degrees Kelvin brightness temperature, the upper scale in column density, assuming a line width of 20 kms^{-1}. The dotted lines show the extrapolation for a velocity limit of -100 kms^{-1}. A linear and a parabolic least-squares fit were made to the corrected observational curves in the range between 0.06 and 0.20 K.

Using UV absorption lines and assuming an element abundance one can probe much lower hydrogen column densities than in the 21-cm emission line. For instance, of the lines that are in the wavelength band of the IUE satellite, SiII $\lambda 1260$ allows to detect material where the hydrogen column is 2×10^{17} cm^{-2}. Therefore (at a velocity limit of $-100\,km\,s^{-1}$) the relation between sky coverage and detection limit has been extrapolated from the survey limit of 10^{18} cm^{-2} down to 10^{17} cm^{-2} as shown by the dotted lines in Fig. 1.

To find the extrapolation a correction of the order of 10% was made for incomplete sky coverage and for the overestimation of sky area in the case of single-point and two-point clouds, as will be described in Wakker 1989a. The extrapolation predicts that at the level of 2×10^{17} cm^{-2} between 25 and 60% of the sky is covered by gas having $v_{lsr} < -100\,km\,s^{-1}$. However, in Danly's (1989) sample there are 19

stars more distant than 1.5 kpc and having $l < 180°$, but in none absorption at velocities more negative than than $-100\,\mathrm{km\,s^{-1}}$ is detected. Unless the HVC's do not contain heavy elements this implies that they, at least statistically, are farther away than 1.5 kpc.

3. Modeling

In order to fully understand the implications of the survey data for the understanding of the origin of HVCs, modeling is necessary. Models have been constructed that are based on the following scheme:

1) Choose a galactic potential.
2) Inject clouds into this potential according to some prescription. A prescription consists of drawing from a given distribution a random radius, azimuth, height, velocity vector and mass at the time of formation.
3) Follow the clouds in their ballistic orbit and in their evolution until the clouds either disperses or is destroyed, for instance when it hits the galactic disk.
4) At each timestep determine the observables (longitude, latitude, LSR velocity, flux, area).

The galactic potential that was chosen consists of a bulge, halo and disk with parameters for the bulge and halo as given by van der Kruit (1986):

$$\rho_{bulge}(R) = \rho_{0,bulge}\left(\frac{R}{b}\right)^{-\frac{3}{2}}\left(1+\frac{R^2}{b}\right)^{-1}, \qquad \rho_{halo}(R) = \rho_{0,halo}\left(1+\frac{R^2}{a}\right)^{-1},$$

with b=300 pc, $\rho_{\odot,bulge}$=0.0002 $\mathrm{M_\odot\,pc^{-2}}$, a=2700 pc and $\rho_{\odot,halo}$=0.008 $\mathrm{M_\odot\,pc^{-2}}$. The halo is cut off at 60 kpc radius. The disk density is given by:

$$\rho_{disk}(r,z) = \rho_{0,disk}\exp-\frac{r}{h}\exp-\frac{z}{s},$$

with radial and vertical scalelengths h=5 kpc and s=325 pc. In order to get a rotation velocity of $220\,\mathrm{km\,s^{-1}}$ at the solar radius (8.5 kpc) the total disk surface density at the sun must be $75\,\mathrm{M_\odot\,pc^{-2}}$.

Cloud evolution is modelled in a very simple way: they are assumed to be pressure confined throughout their lifetime and therefore always stay the same size. Only when they hit the gaseous disk are they assumed to be destroyed. At formation a mass is given to each cloud, chosen from a power-law spectrum with slope α. Assuming the same average density for all clouds makes it possible to calculate the cloud radius. Together with the cloud distance this allows to calculate the cloud flux, brightness temperature and area. By comparing the observed distributions of flux and area with the model distributions it follows that $\alpha = -1.5$ and that the density, averaged across the whole cloud, must be about $0.01\,\mathrm{cm^{-3}}$.

The different types of models are characterized by different presciptions for the injection scheme. Various possibilities exist, three of which will be described here.

1) The cannonball model: Clouds form in the galactic disk and are corotating. They also get a vertical velocity of 50 $\mathrm{km\,s^{-1}}$. Such a model describes e.g. gas directly ejected from the disk by means of supernova explosions.

2) The galactic fountain model: As suggested by Bregman (1980) the HVCs with velocities up to 200 $\mathrm{km\,s^{-1}}$ may consist of cooled halo gas. The prescription used here to parametrize this fountain model is the following: the radial density distribution is exponential with scalelength 5 kpc (like the galactic disk) and radius 15 kpc); condensation takes place at heights between 2 and 6 kpc above the disk; the vertical velocity at formation is a random value between -75 and $+75$ $\mathrm{km\,s^{-1}}$; the component in the direction of galactic rotation is determined from an estimate of the radius at which the hot gas rose up by assuming that it moved upward and outward by one scalelength in both r and z ($h_r = \frac{kT}{\mu g_r(r_{form})}, h_z = \frac{kT}{\mu g_z(r_{form})}$) and assuming conservation of angular momentum.

3) The infall model: Clouds form outside the galactic disk at distances up to 150 kpc, having a r^{-2} density distribution. The velocity distribution is found by taking the first and second moments of the radial velocities of all dwarf galaxies in the list of Richter *et al.* (1987) nearer than 300 kpc. Assuming that the azimuthal dispersions are equal to the radial dispersion, this gives the clouds a velocity dispersion of 50 $\mathrm{km\,s^{-1}}$ in all directions and an infall component of -20 $\mathrm{km\,s^{-1}}$.

In Figure 2 the observed distribution of HVCs in longitude and LSR velocity is shown, together with the predictions obtained from the first runs of the three described models. From the comparison of the observed distribution with the model pictures it is immediately clear that none of the models can completely explain the data. The fact that at longitudes below 180° mostly negative velocities are observed and above 180° mostly positive velocities is clearly seen in the models, however. This is due to the reflection of the rotation of the sun around the galactic center. In the infall model clouds with velocities up to 400 $\mathrm{km\,s^{-1}}$ are seen, but on the whole the density distribution of points is not what is observed. The cannonball and fountain models show the concentration of clouds at velocities between $+/-100$ and $+/-200$ $\mathrm{km\,s^{-1}}$, but are unable to explain the existence of clouds with higher velocities and of the HVCs in the anticenter region. A more complete description of models and conclusions will be presented by Wakker & Bregman (1989).

4. High-resolution observations

Since Schwarz & Oort (1981) published the first high-resolution map of a HVC, a large number of new fields has been observed at Westerbork, with integration times of $2\mathrm{x}12^h$ and $4\mathrm{x}12^h$. Six of these fields have been completely reduced. A full description of the datataking, reduction, analysis and the data themselves will be presented by Wakker (1989b).

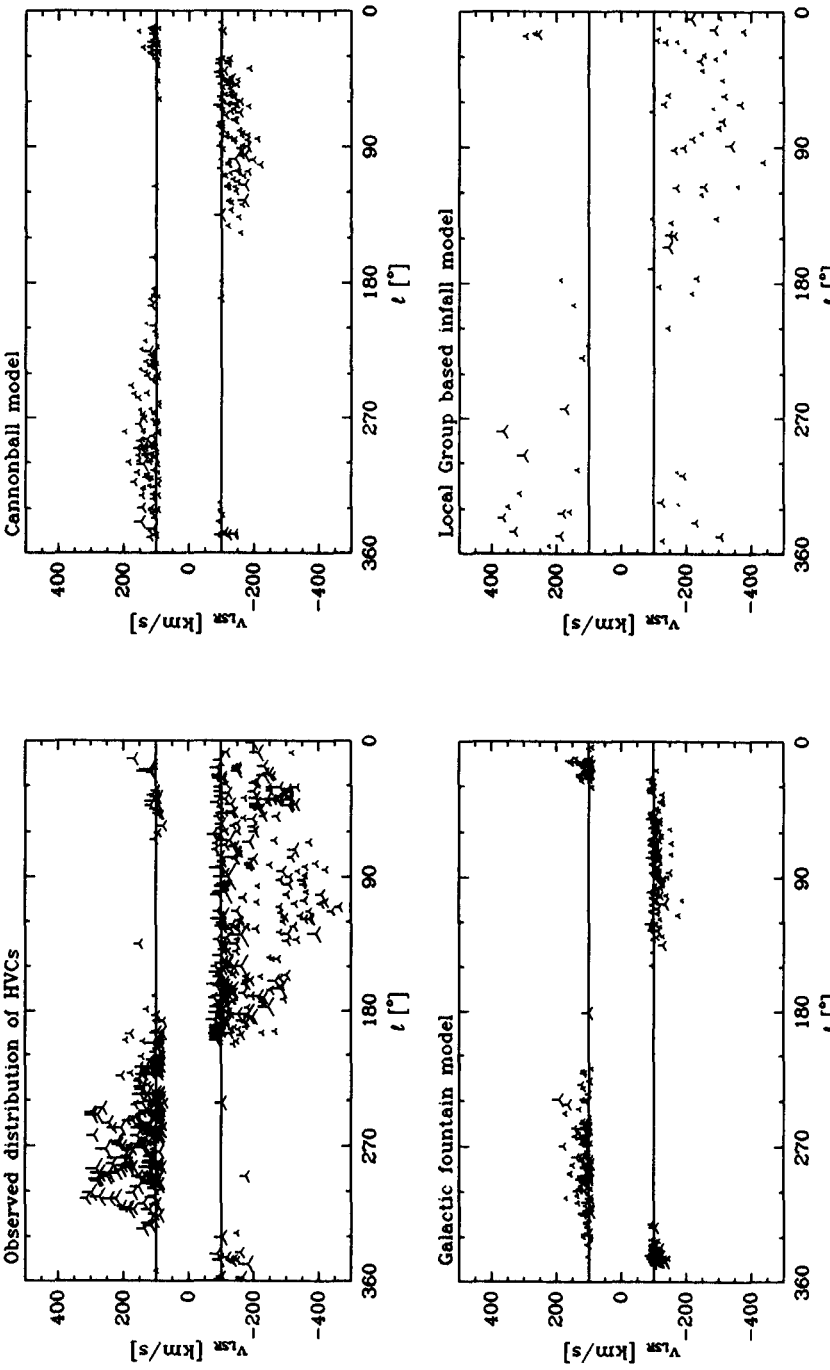

Fig. 2. Observed and predicted distribution in longitude and LSR velocity of HVCs. The model parameters are described in the text. The size of the symbols is proportional to the cloud flux.

4.1 Fine structure

In Fig. 3 a representative total-hydrogen map of a HVC is presented. Immediately apparent is the existence of much fine structure. It can be shown that even with a beam of 1′ the smallest concentrations are not completely resolved. This means that there is structure in the gas at linear scales less than 0.3 D(kpc) parsec (with D the cloud distance).

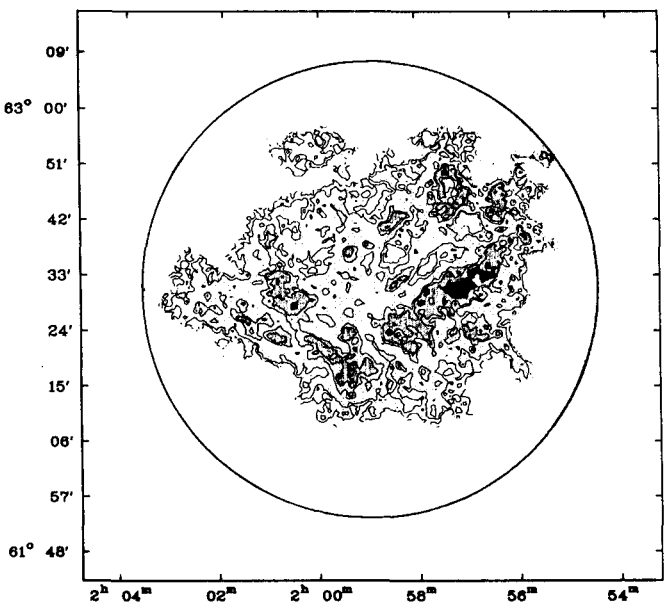

Figure 3. Total hydrogen map of HVC131+1-200 as observed by the WSRT. Contours and gray scales are at the level of 5, 10, 15, 20 and 25×10^{18} cm^{-2}. The beam is 1′. The circle indicates the radius where the primary beam attenuation is a factor 2.

The density contrast can be as high as 5 on scales of 3′. For the absorption-line studies of galactic halo gas this introduces a considerable uncertainty in the derivation of abundances. A small feature which lies right along the line of sight to a halo star may provide a strong absorption component but go undetected in a single-dish beam due to beam-dilution effects. Alternatively, a cloud seen in HI but not in absorption could in fact lie in front of the probe star, but sufficiently filamentary or patchy that the bulk of the gas lies just off the line of sight from the pencil-beam to the star.

4.2 Line widths and spin temperature of the gas

At each of the positions in the WSRT data cubes a gaussian fit was made to the spectrum of the clouds. Usually only one component is present, but profiles with 2 or even 3 components are not rare. From the fit one obtains the velocity field of the cloud and the line width of its profiles.

The two VHVCs that have been observed (HVC114-10-440 and HVC110-7-465) give a surprising result. They have very different line widths (FWHM 2.1 and 17.5 $km\,s^{-1}$ respectively), although they are only 5 degrees apart on the sky and have similar spatial structure (both at high resolution and in the single-dish observations by Cohen & Mirabel (1979)). The single-dish data already suggested this: for HVC110-7-465 the profiles had an FWHM of 23 $km\,s^{-1}$, while HVC114-10-440 showed an envelope with FWHM 23 $km\,s^{-1}$ and a core with FWHM 7 $km\,s^{-1}$. At high-resolution HVC110-7-465 still does not show narrow profiles, but for HVC114-10-440 only extremely narrow ones are seen close to the velocity resolution of the data. It can be shown that because there exists a large velocity gradient across the field, the wider lines are due to beam-smearing. A possible explanation for the difference between the two clouds may be that they are both in a cooling stage, but HVC110-7-465 has not yet cooled as far as the other one. This would provide evidence for a hot origin of the VHVCs. On the other hand, both objects may have been intergalactic gas clouds being accelerated by the Galaxy and now are in the process of being disrupted by friction with halo gas. In this picture HVC114-10-440 is still in its original cool state, while in the other HVC a substantial amount of heat has already been generated.

In the other four fields the fitted linewidths are rather small: 3 $km\,s^{-1}$. Such narrow widths imply that the kinetic temperature of the gas is below 200 K. A lower limit of 30 K is provided by the peak brightness temperature, thereby considerably narrowing the previously known limits to the temperature. No evidence is found for broad lines, indicative of hot gas, although these might be hidden in the smooth background which has been filtered out by the interferometer. However the broad lines seen with single-dish instruments are likely to be due to beam-smearing effects.

References

Bajaja E., de Cappa Nicolau C.E., Cersosimo J.C., Loiseau N., Martin M.C., Morras R., Olano C.A., Poppel W.G.L., 1985, *Astrophys. J. Suppl. Ser.* **58**, 143

Bregman J.N., 1980, *Astrophys. J.* **236**, 577

Cohen R.J., Mirabel I.F., 1979, *Monthly Notices Roy. Astr. Soc.* **186**, 217

Danly L., 1989, *Astrophys. J.* **342**, ..

Giovanelli R., 1980, *Astron. J.* **85**, 1155

Giovanelli R., Haynes M.P., 1976, *Monthly Notices Roy. Astr. Soc.* **177**, 525

Giovanelli R., Verschuur G.L., Cram T.R., 1973, *Astron. Astrophys.* **12**, 209

Hulsbosch A.N.M., Wakker B.P., 1988, *Astron. Astrophys. Suppl. Ser.* **71**, 191

van der Kruit, P.C., 1986, in "The Galaxy", NATO ASI series, ed. G.Gilmore and B.Carswell, p27

Richter O.G., Tammann G.A., Huchtmeier W.K., 1987, *Astron. Astrophys.* **171**, 33

Schwarz U.J., Oort J.H., 1981, *Astron. Astrophys.* **101**, 305

Wakker B.P., 1989a, in preparation

Wakker B.P., 1989b, in preparation

Wakker B.P., Bregman J.N., 1989, in preparation

Discussion:

VAN WOERDEN: Do your small velocity dispersions (1-2 kms^{-1}) and consequent low temperatures (~200K) apply only to the dense concentrations, or also to the thinner gas in between?

WAKKER: In the less dense regions the fitted dispersions are also low, but the accuracy with which they can be measured is less because the signal to noise is less.

MEBOLD: Calculating your temperature limits, did you have the zero-spacing HI emission added to your data? It has been found that the spatially more extended HI emission tends to have the larger velocity dispersion.

WAKKER: I did not add in the zero and short-spacing information. And from comparing with single-dish data it is clear that a significant amount of flux is missing. Without really going through the process of adding short-spacing to the maps it is impossible to know exactly the linewidths of this "missing" flux. However, because the linewidths measured from the WSRT maps increase when you smooth them and because the interferometer filters out only low spatial frecuencies, not low spectral frecuencies, I think that it is not likely that the smooth background has broad lines. The two-component structure seen in single-dish maps at 10' resolution could be the result of beam-smearing, because there are large velocity gradients and jumps in the cloud. In one particular case (HVC 114-10-440) I could reproduce the 2-component shape of the single-dish profile by adding all the profiles fitted at 1' resolution, all of which had an FWHM of only about 1 kms^{-1}.

HEILES: Did you try to do a 21cm absorption experiment using radio continuum sources?

WAKKER: I once correlated a catalogue of 21-cm radio sources with the Dwingeloo survey of HVCs. Unfortunately none of the strong continuum sources fell on top of an appreciable HVC component. And if you try to make a prediction of the absorption strength for the correlating sources, only a few are expected to give an absorption of more than 3 sigma. Clearly it is necessary to get a more complete catalogue of 21cm sources and to do the correlation again, and also to use long integration times on the candidate sources.

de BOER : In particular the WSRT data that you showed are very nice and extremely important. But by gost, I wished you had not shown it since it makes clear how difficult a task the halo-absorption line people have!

WAKKER: That certainly is true. There are large variations of integrated column density on scales of just a few arcminutes. But of course, in the WSRT maps the short-spacing information is missing and it is known that the integrated flux calculated from the WSRT maps is between 50 and 80% of the single-dish flux so that there must be a smooth background present in addition to all the fine structure. This might help to get a measurable column density toward the star.

DANLY: I cannot determine the contrast scale in your slide (of the high spatial resolution HVC observations). Is there sufficient structure over scales of 2 arcmin to account for the differences seen in the 50 kms^{-1} Na components toward SN1987a and Sk-69 203, as shown in the previous talk?

WAKKER: The contrast in the WSRT maps is quite high. Certainly on scales of 5 arcmin the intensity can drop from a high value to alm ost nothing. On 2 arcmin scales the contrast is about a factor 3. So, I think this can easily explain the difference in the Na lines seen toward the LMC.